

# SCIENTIFIC REPORTS



OPEN

## Meta-analysis of brain iron levels of Parkinson's disease patients determined by postmortem and MRI measurements

Received: 29 February 2016  
Accepted: 19 October 2016  
Published: 09 November 2016

Jian-Yong Wang<sup>1,2,\*</sup>, Qing-Qing Zhuang<sup>1,\*</sup>, Lan-Bing Zhu<sup>1</sup>, Hui Zhu<sup>1</sup>, Ting Li<sup>1</sup>, Rui Li<sup>2</sup>, Song-Fang Chen<sup>1</sup>, Chen-Ping Huang<sup>2</sup>, Xiong Zhang<sup>1</sup> & Jian-Hong Zhu<sup>2,3</sup>

Brain iron levels in patients of Parkinson's disease (PD) are usually measured in postmortem samples or by MRI imaging including R2\* and SWI. In this study we performed a meta-analysis to understand PD-associated iron changes in various brain regions, and to evaluate the accuracy of MRI detections comparing with postmortem results. Databases including Medline, Web of Science, CENTRAL and Embase were searched up to 19<sup>th</sup> November 2015. Ten brain regions were identified for analysis based on data extracted from thirty-three-articles. An increase in iron levels in substantia nigra of PD patients by postmortem, R2\* or SWI measurements was observed. The postmortem and SWI measurements also suggested significant iron accumulation in putamen. Increased iron deposition was found in red nucleus as determined by both R2\* and SWI, whereas no data were available in postmortem samples. Based on SWI, iron levels were increased significantly in the nucleus caudatus and globus pallidus. Of note, the analysis might be biased towards advanced disease and that the precise stage at which regions become involved could not be ascertained. Our analysis provides an overview of iron deposition in multiple brain regions of PD patients, and a comparison of outcomes from different methods detecting levels of iron.

Iron overload has been implicated in the pathology and pathogenesis of Parkinson's disease (PD). The substantia nigra, where the selective loss of dopaminergic neurons occurs, is the primary region in the brain known to deposit iron. Additionally, aberrant iron concentrations have been observed in other brain regions such as red nuclei, globus pallidus and cortex of PD patients, despite of unknown pathology<sup>1-3</sup>. Spectroscopic analyses of postmortem brains display an increased iron levels in the substantia nigra, which has been suggested to correlate with the severity of PD<sup>2,4</sup>. In recent decades, advancements in imaging techniques, such as magnetic resonance imaging (MRI), have contributed to an enhanced understanding of the pathological progression and clinical diagnosis of PD. Consequently, iron load may be estimated in a non-invasive manner using R2/R2\* relaxometry (with better results obtained using R2\*<sup>5-7</sup>) and, more recently, susceptibility-weighted imaging (SWI). Nonetheless, while largely consistent and reproducible results can be obtained in many experiments these techniques are not yet fully validated<sup>8</sup>.

In this study, we extracted results of iron analyses employing postmortem brains and R2\* and SWI methods from the literature, and performed a systematical meta-analysis aiming to 1) confirm the iron overload observation in the substantia nigra, 2) explore other regions of the brain carrying different levels of iron, and 3) evaluate to what extent these two MRI methods correlate with the measurements of postmortem brains. Meanwhile, as detailed in the discussion section, several limitations are disclosed in an attempt to fully understand the scope of this meta-analysis, such that the disease severity was not differentiated due to insufficient information during data extraction that may affect outcomes of MRI imaging.

<sup>1</sup>Department of Neurology, the Second Affiliated Hospital, Wenzhou Medical University, Wenzhou, Zhejiang 325000, China. <sup>2</sup>Department of Preventive Medicine, Wenzhou Medical University, Wenzhou, Zhejiang 325035, China. <sup>3</sup>Key Laboratory of Watershed Science and Health of Zhejiang Province, Wenzhou Medical University, Wenzhou, Zhejiang 325035, China. \*These authors contributed equally to this work. Correspondence and requests for materials should be addressed to C.P.H. (email: hcp@wmu.edu.cn) or X.Z. (email: zhangxiong98@gmail.com) or J.H.Z. (email: jhzhu@wmu.edu.cn)

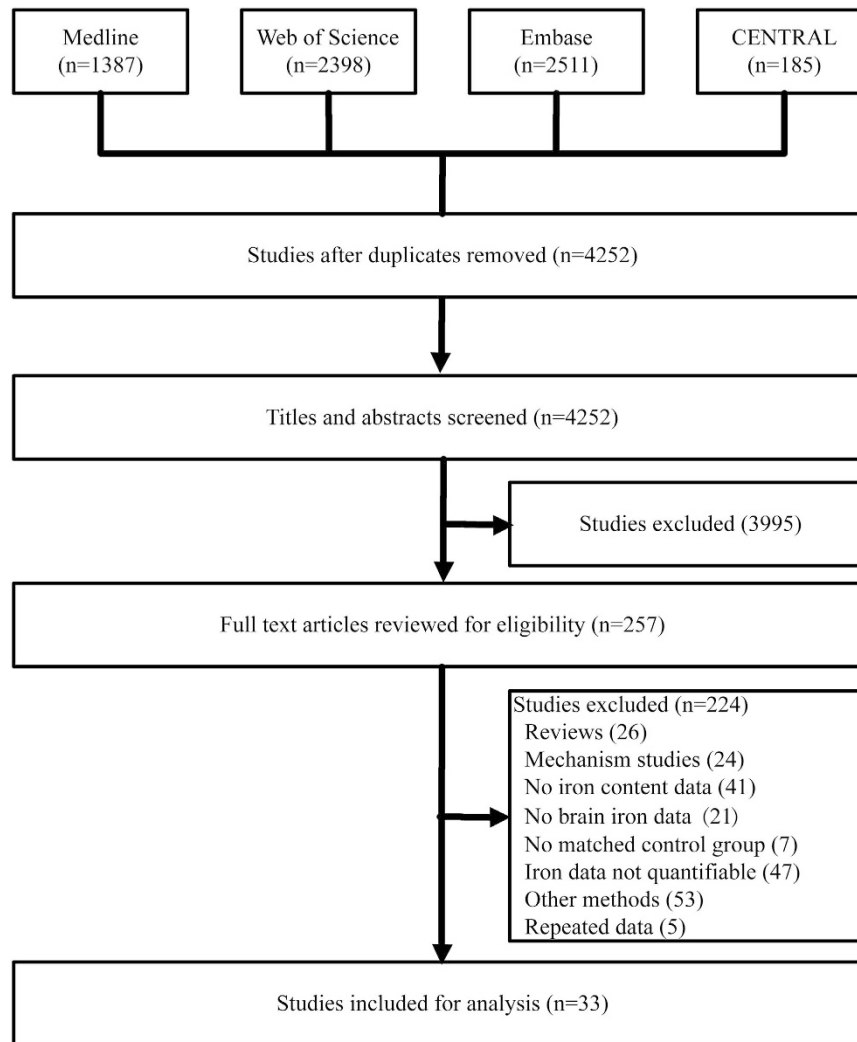


**Figure 1.** Flow chart describing the selection process of articles retrieved from initial literature search. CENTRAL, Cochrane Central Register of Controlled Trials.

## Results

**Search Results.** The initial search using the keywords as described in the method section returned a total of 4252 articles (Fig. 1). A subsequent screening of the titles and abstracts reduced the number to 257. Following an exhaustive examination of the contents, 224 articles were excluded according to the selection criteria detailed in the method section. Of the 33 articles being selected that report iron content (summarized in Table 1), 11 of them employed postmortem analyses<sup>2,4,9–17</sup>, 14 were measured by R2\*<sup>3,18–30</sup> and 8 by MRI relaxometry SWI<sup>31–38</sup>. The disease comorbidity and diagnostic performance of the cohorts of these 33 studies are summarized in Table S1.

**Quality Assessment.** Quality assessment by Newcastle-Ottawa Scale suggested four-stars or above out of a maximum of nine for all of the 33 publications. The detailed quality assessment is listed in Table 1.

**Postmortem comparison of iron concentration in defined brain regions.** Eleven of the manuscripts examined iron concentration in seven regions of postmortem brains. The numbers of subjects for each region were 98 (frontal lobe), 44 (temporal lobe), 117 (nucleus caudatus), 104 (globus pallidus), 173 (substantia nigra), 100 (putamen), and 58 (cerebellum). Although iron concentration was significantly increased in the substantia nigra of PD patients (WMD = 39.85, 95% CI, 8.06–71.65,  $p = 0.01$ ; Fig. 2E), significant heterogeneity was detected in these cohorts ( $I^2 = 71\%$ ;  $p = 0.0006$ ). Subsequent sensitivity analysis suggested that such heterogeneity was attributed to the study of Griffiths *et al.*<sup>11</sup>. Further analysis that eliminated this study ( $I^2 = 12\%$ ;  $p = 0.33$ ) also showed a significant increase of iron concentration in the substantia nigra (WMD = 23.60, 95% CI = 7.62–39.58,  $p = 0.004$ ; Fig. 2F). Additionally, increased iron levels were observed in the putamen of PD subjects (WMD = 19.30, 95% CI = 7.24–31.36,  $p = 0.002$ ,  $I^2 = 4\%$ ; Fig. 2G). No significant differences were observed in other brain regions (Fig. 2). The funnel plots analyzing publication bias appeared to be symmetric by visual inspection (Fig. 3).

Article	Healthy controls			PD patients			PD diagnosis	Detection	Method type	UPDRS score	UPDRS motor score	H-Y scale	Disease duration	Publication Quality Assessment
	n	Age <sup>a</sup>	Gender (F/M)	n	Age <sup>a</sup>	Gender (F/M)								
Yu <i>et al.</i> <sup>17</sup>	10	84.6 ± 1.5	6/4	10	82.7 ± 1.7	4/6	UK PD Brain Bank criteria	ICP	Postmortem	—	—	—	—	*****
Loeffler <i>et al.</i> <sup>12</sup>	8	74.6 ± 7.6	4/4	14	74.9 ± 8.7	5/9	Pathological examination	COL	Postmortem	—	—	—	—	****
Griffiths <i>et al.</i> <sup>11</sup>	6	83.3 ± 2.1	—	6	83.6 ± 2.4	—	Pathological examination	AA	Postmortem	—	—	—	—	*****
Dexter <i>et al.</i> <sup>2</sup>	34	81.3 ± 1.5	21/13	27	74.9 ± 1.4	11/16	Clinical and pathological examination	ICP	Postmortem	—	—	—	—	****
Riederer <i>et al.</i> <sup>4</sup>	4	73 (68–78)	3/1	13	76 (68–82)	7/6	Pathological examination	SPH	Postmortem	—	—	—	—	*****
Sofic <i>et al.</i> <sup>13</sup>	8	75.3 (66–86)	4/4	8	71.3 ± 12.5	4/4	Pathological examination	SPH	Postmortem	—	—	—	7.5 ± 3.4	*****
Visanji <i>et al.</i> <sup>15</sup>	3	62.7 (47–78)	1/2	3	69.3 (56–79)	1/2	Pathological examination	AA	Postmortem	—	—	—	21 ± 3.8	*****
Wypijewska <i>et al.</i> <sup>16</sup>	29	61–85	—	17	61–85	—	Clinical and pathological examination	MS	Postmortem	—	—	—	—	*****
Galazka-Friedm <i>et al.</i> <sup>10</sup>	8	64 ± 6	—	6	70 ± 4	—	Clinical and pathological examination	MS	Postmortem	—	—	4–5	4–7	****
Uitti <i>et al.</i> <sup>14</sup>	12	70	4/8	9	73	3/6	Pathological examination	AA	Postmortem	—	—	—	—	****
Chen <i>et al.</i> <sup>9</sup>	6	—	—	10	—	—	—	AA	Postmortem	—	—	—	—	****
Gorell <i>et al.</i> <sup>18</sup>	10	60.0 ± 8.7	5/5	13	65.2 ± 12.7	2/11	Clinical diagnosis	3T	R2*	—	—	1.5–3.0	3–13	*****
Graham <i>et al.</i> <sup>19</sup>	25	64.0 ± 6.6	6/7	21	61.4 ± 7.3	10/11	UK PD Brain Bank criteria	1.5T	R2*	—	—	—	11.1 ± 4.5	*****
Martin <i>et al.</i> <sup>20,b</sup>	11	55.9 ± 7.3	4/7	22	61.9 ± 9.0	8/14	Published criteria <sup>66</sup>	3T	R2*	—	16.7 ± 7.1	—	3.2 ± 1.7	*****
				19	60.3 ± 8.4	6/13				—	16.9 ± 7.5	—	2.9 ± 1.6	
Du <i>et al.</i> <sup>21</sup>	29	59.6 ± 6.7	17/12	40	60.7 ± 8.3	17/23	Published criteria <sup>66</sup>	3T	R2*	—	23.4 ± 15.2	1.8 ± 0.6	4.2 ± 4.7	*****
Bunzeck <i>et al.</i> <sup>22</sup>	20	66.0 ± 9.1	10/10	20	66.3 ± 9.0	9/11	Queens Square Brain Bank criteria <sup>67</sup>	3T	R2*	34.6 ± 17.4	—	—	—	*****
Lee <i>et al.</i> <sup>23</sup>	21	60.0 ± 6.1	9/12	29	59.1 ± 7.6	12/17	UK PD Brain Bank criteria	3T	R2*	—	25.5 ± 9.2	2.05 ± 0.5	2.5 ± 1.9	*****
Lewis <i>et al.</i> <sup>3</sup>	23	59.9 ± 7.0	17/12	38	60.6 ± 8.0	17/23	Published criteria <sup>66</sup>	3T	R2*	—	23.8 ± 15.4	1.8 ± 0.6	4.4 ± 4.7	****
Rossi <i>et al.</i> <sup>24</sup>	21	66 (58–80)	17/4	37	69 (42–86)	18/19	Clinical diagnosis	3T	R2*	—	—	—	—	****
Ulla <i>et al.</i> <sup>25</sup>	26	57.0 ± 8.5	17/9	27	60.2 ± 10.7	14/13	PD Society Brain Bank <sup>68</sup>	1.5T	R2*	—	12.1 ± 8.5	1.9 ± 0.7	5.7 ± 4.4	*****
Rossi <i>et al.</i> <sup>26</sup>	19	65 (58–80)	15/4	25	73 (44–87)	14/11	Clinical diagnosis	3T	R2*	—	—	—	—	****
Barbosa <i>et al.</i> <sup>27</sup>	30	64 ± 7	21/9	20	66 ± 8	8/12	UK PD Brain Bank criteria	3T	R2*	—	—	2.3 ± 0.6	8.1 ± 4.2	*****
Murakami <i>et al.</i> <sup>30</sup>	21	69.7 ± 8.6	12/9	21	72.0 ± 7.5	12/9	UK PD Brain Bank criteria	3T	R2*	—	—	2 (1–3)	2.7 ± 2.3	****
He <i>et al.</i> <sup>29</sup>	35	60.5 ± 6.5	14/21	44	58.0 ± 8.8	19/25	UK PD Brain Bank criteria	3T	R2*	—	15.6 ± 6.2	1.4 ± 0.5	2.8 ± 1.6	****
Du <i>et al.</i> <sup>28</sup>	47	62.2 ± 8.8	24/23	47	65.8 ± 10.1	25/22	UK PD Brain Bank criteria	3T	R2*	39.6 ± 24.8	21.8 ± 15.2	—	5.5 ± 4.8	****
Zhang <i>et al.</i> <sup>34</sup>	26	57.3 ± 11.6	12/14	40	58.7 ± 12.8	19/21	UK PD Brain Bank criteria	3T	SWI	—	19.0 ± 7.8	—	3.6 ± 2.9–	*****
Jin <i>et al.</i> <sup>35</sup>	45	55.4 ± 14.9	19/26	45	56.3 ± 10.9	14/31	UK PD Brain Bank criteria	3T	SWI	15.1 ± 9.3	12.0 ± 7.1	—	—	*****
Wang <i>et al.</i> <sup>32</sup>	14	64.3 ± 12.7	7/7	20	67.2 ± 10.7	10/10	Clinical diagnosis	3T	SWI	—	—	—	2.8 ± 2.8	*****
Wang <i>et al.</i> <sup>37</sup>	44	59.4 ± 11.8	23/21	16	63.3 ± 10.6	7/9	UK PD Brain Bank criteria	1.5T	SWI	—	—	—	2.5 ± 1.7	****
Han <i>et al.</i> <sup>31</sup>	20	55.9 ± 6.2	8/12	15	57.4 ± 7.1	8/7	UK PD Brain Bank criteria	3T	SWI	23.0 ± 5.6	—	2.2 ± 0.5	2.5 ± 1.6	****
Kim <i>et al.</i> <sup>36</sup>	25	56.2 ± 6.5	13/12	30	57.6 ± 6.8	11/19	UK PD Brain Bank criteria	3T	SWI	—	24.5 ± 8.4	1.7 ± 0.5	1.7 ± 1.1	****
Wu, <i>et al.</i> <sup>33</sup>	40	66.5 ± 6.0	18/22	54	65.6 ± 5.8	21/33	UK PD Brain Bank criteria	3T	SWI	—	—	≥1.5	—	****
Huang, <i>et al.</i> <sup>38</sup>	19	65.0 ± 9.0	—	30	68.0 ± 9.0	6/24	—	3T	SWI	—	—	—	—	****

**Table 1. Characteristics of the 33 studies included for meta-analyses.** <sup>a</sup>Data in this column are presented as mean ± SD or Range or Median (Range) or Mean (Range) or the detail ages; <sup>b</sup>In this study the patient group with n = 22 is for mid-brain images including substantia nigra and red nucleus, and the one with n = 19 is for forebrain images including globus pallidus, putamen, nucleus caudatus, and white matter. UPDRS, Unified Parkinson's Disease Rating Scale; H-Y, Hoehn and Yahr; ICP, inductively coupled plasma spectroscopy; COL, colorimetry; AA, atomic absorption; SPH, spectrophotometry; MS, Mössbauer spectroscopy.

**MRI comparison of iron concentration in defined brain regions.** Fourteen articles were included in the R2\* subgroup of meta-analyses in seven brain regions. The total subject numbers were 437 (nucleus caudatus), 500 (globus pallidus), 631 (substantia nigra), 446 (putamen), 265 (red nucleus), 117 (white matter) and 182 (thalamus). In the substantia nigra of PD subjects, iron content was elevated (WMD = 3.81, 95% CI = 2.59–5.02,  $p < 0.00001$ ) despite of a relatively high heterogeneity ( $I^2 = 59%$ ,  $p = 0.005$ ; Fig. 4C). Results of a sensitivity analysis ascribed the heterogeneity to the studies of Ulla *et al.*<sup>25</sup> and Gorell *et al.*<sup>18</sup>, as exclusion of them eliminated the

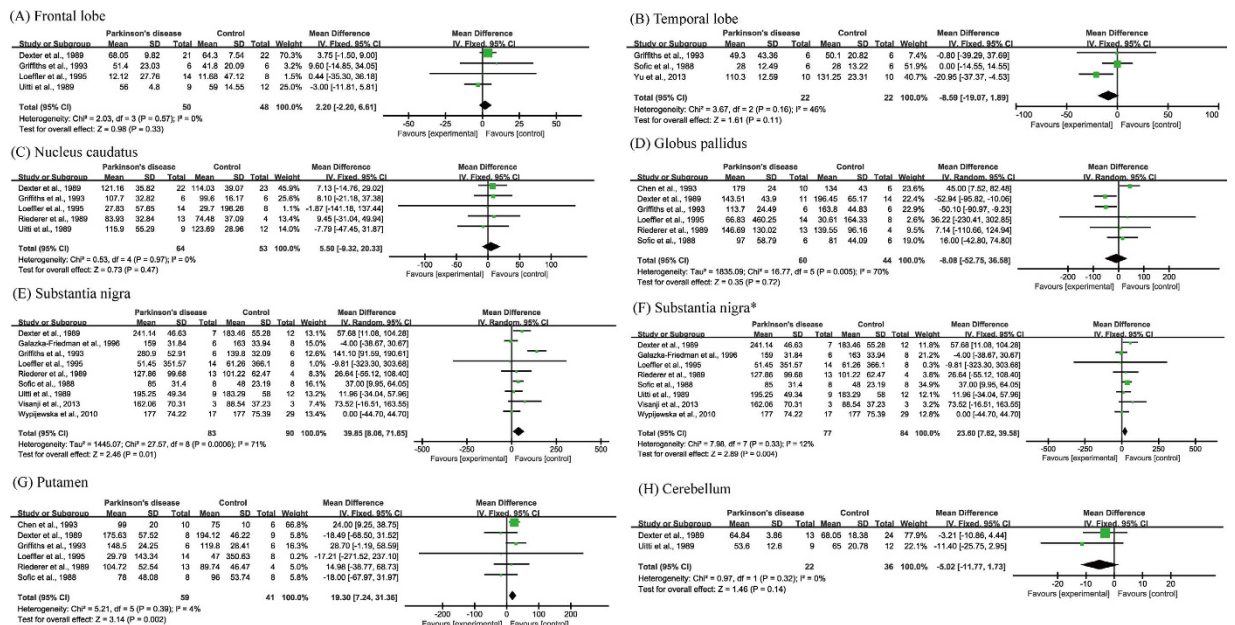


**Figure 2. Statistical summaries and forest plots of studies comparing iron concentrations by postmortem analysis. (D,E) Pooled using random-effects models. The others were pooled using fixed-effects models. \* Analyzed after heterogeneity was removed.**

heterogeneity ( $I^2 = 0\%$ ,  $p = 0.49$ ; Fig. 4D). Subsequent meta-analysis again demonstrated a significant increase of iron concentration in the substantia nigra ( $WMD = 3.91$ ,  $95\% \text{ CI} = 3.05\text{--}4.77$ ,  $p < 0.00001$ ; Fig. 4D). Iron concentration was significantly increased in the red nucleus ( $WMD = 1.93$ ,  $95\% \text{ CI} = 0.70\text{--}3.17$ ,  $p = 0.002$ ,  $I^2 = 0\%$ ; Fig. 4F), but not in other brain regions (Fig. 4). The publication biases were acceptable as determined by funnel plots (Fig. 5).

Eight articles were included in the SWI subgroup of meta-analyses in seven brain regions. The total subject numbers were 431 (nucleus caudatus), 431 (globus pallidus), 431 (putamen), 306 (thalamus), 465 (substantia nigra), 465 (red nucleus) and 211 (white matter). A significant increase in iron concentration was observed in the substantia nigra ( $WMD = 6.5$ ,  $95\% \text{ CI} = 3.31\text{--}9.68$ ,  $p < 0.0001$ ) with high heterogeneity ( $I^2 = 94\%$ ,  $p < 0.0001$ ; Fig. 6D). Significant increases in iron concentration were also shown in the nucleus caudatus ( $WMD = 0.81$ ,  $95\% \text{ CI} = 0.37\text{--}1.25$ ,  $p = 0.0003$ ,  $I^2 = 24\%$ ; Fig. 6A), putamen ( $WMD = 1.03$ ,  $95\% \text{ CI} = 0.06\text{--}2.01$ ,  $p = 0.04$ ,  $I^2 = 60\%$ ; Fig. 6E), and red nucleus ( $WMD = 0.85$ ,  $95\% \text{ CI} = 0.15\text{--}1.54$ ,  $p = 0.02$ ,  $I^2 = 44\%$ ; Fig. 6H). When the article of Wang *et al.*<sup>37</sup> was removed based on sensitivity analysis, we still observed an increase of iron concentration in the putamen ( $WMD = 0.82$ ,  $95\% \text{ CI} = 0.33\text{--}1.30$ ,  $p = 0.001$ ,  $I^2 = 0\%$ ; Fig. 6F). Significant heterogeneity ( $I^2 = 87\%$ ,  $p < 0.00001$ ) was detected in the globus pallidus group (Fig. 6B), which was attributed to Han *et al.*<sup>31</sup> as determined by a sensitivity analysis. Meta-analysis after exclusion of this paper showed a significant increase of iron concentration in the globus pallidus ( $WMD = 1.76$ ,  $95\% \text{ CI} = 0.98\text{--}2.54$ ,  $p < 0.0001$ ,  $I^2 = 0\%$ ; Fig. 6C). The publication biases were acceptable as determined by funnel plots (Fig. 7).

**Structure by structure analyses of results from individual studies and meta-analyses.** It is known that inferences can be particularly prone to Type-I error in studies based on a small number of papers, especially with a small sample size<sup>39</sup>. Therefore, we herein elaborated on the results reported in each study combining the results of meta-analyses and the methodological factors that could have contributed to discrepancies in a brain structure-based fashion.

**Substantia nigra.** As expected, an elevation of iron concentration was found in the substantia nigra in all the three types of measurements (Table 2). This was in line with the majority of the 29 articles we analyzed. Except for the three that did not show a change in postmortem samples<sup>10,12,16</sup>, the other 26 articles reported a trend toward or a statistically significant increase in iron content in the substantia nigra regardless of the type of measurement (postmortem, SWI or R2\*). As a note, three postmortem iron analyses<sup>12,14,16</sup> indicated that the pars compacta and reticulata were not discriminated during the measurement, while the other six studies did not state the relevant information to make this determination.

**Putamen.** Both postmortem and SWI meta-analyses showed an iron overload in PD patients. However, when individual articles describing postmortem samples were analyzed, we found that only one study reported a significant increase in iron content<sup>9</sup>, while the other five were completely negative with mixed trends<sup>2,4,11–13</sup>. Although the results of our meta-analysis suggested a significant increase in iron content in the putamen of PD patients in postmortem samples, caution should be taken in the interpretation of these results as one positive study<sup>9</sup> dominated the other five negative ones in the analysis (Fig. 2G). For SWI, an iron overload was suggested in the putamen based on both random

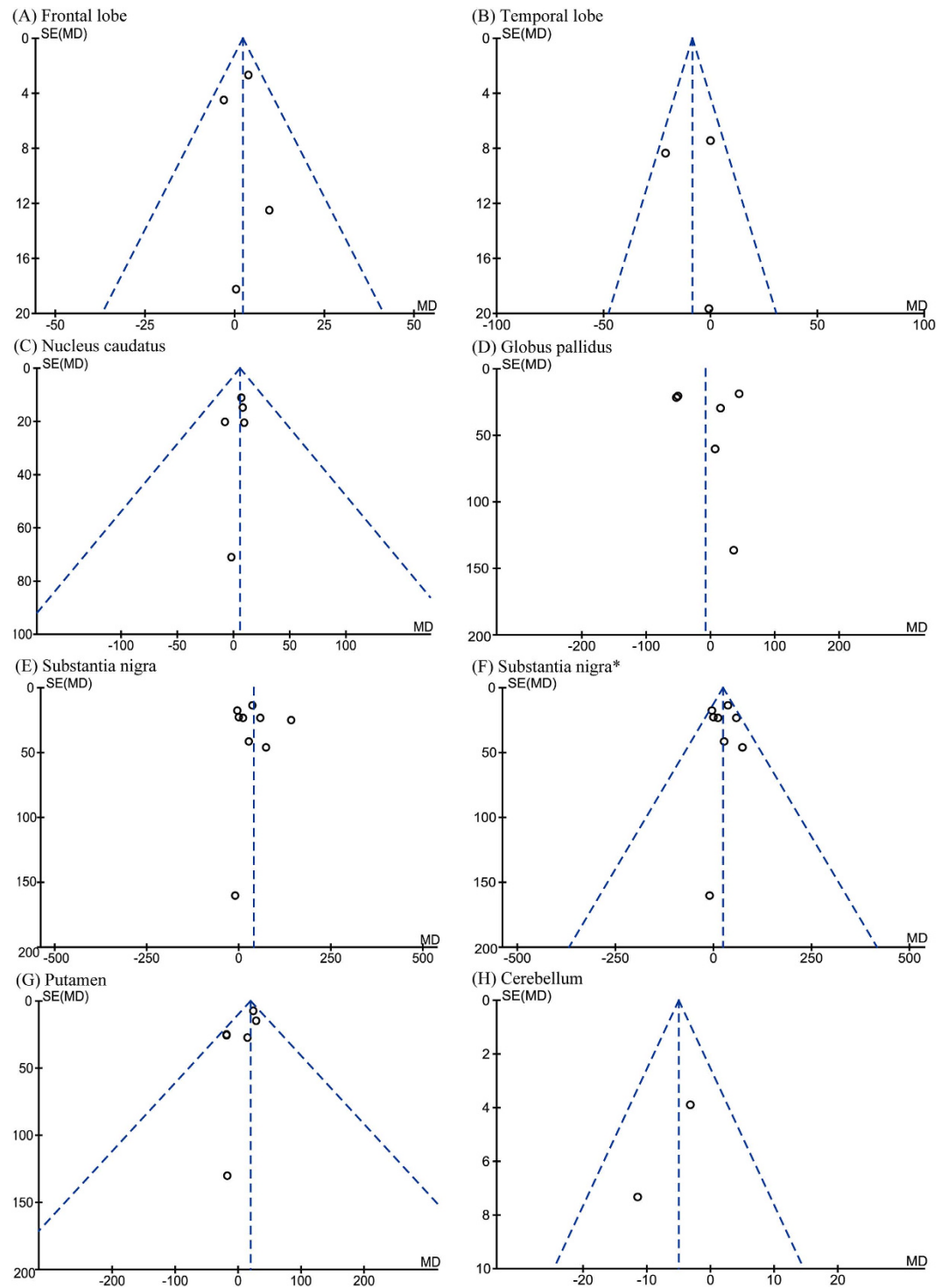


**Figure 3.** Funnel plots that examine possible publication bias in the studies by postmortem analysis.

\*Analyzed after heterogeneity was removed.

and fixed effects models. Results of two independent studies showed elevated iron content in this structure<sup>31,37</sup>, whereas the other five were not significantly different<sup>33–36,38</sup>. One of the positive studies<sup>37</sup> was removed following a sensitivity analysis, and the remaining one<sup>31</sup> drove half of the total effect size thereafter in the fixed effects model (Fig. 6F). Taken together, additional studies are needed to confirm iron accumulation in the putamen.

**Globus pallidus.** For SWI, results of six studies suggested a trend toward, or a significant, increase in the level of iron<sup>33–38</sup>, while one showed a decrease in iron content<sup>31</sup>, which was later removed based on a sensitivity analysis. The subsequent meta-analysis returned a significant increase of iron content in the globus pallidus. However,

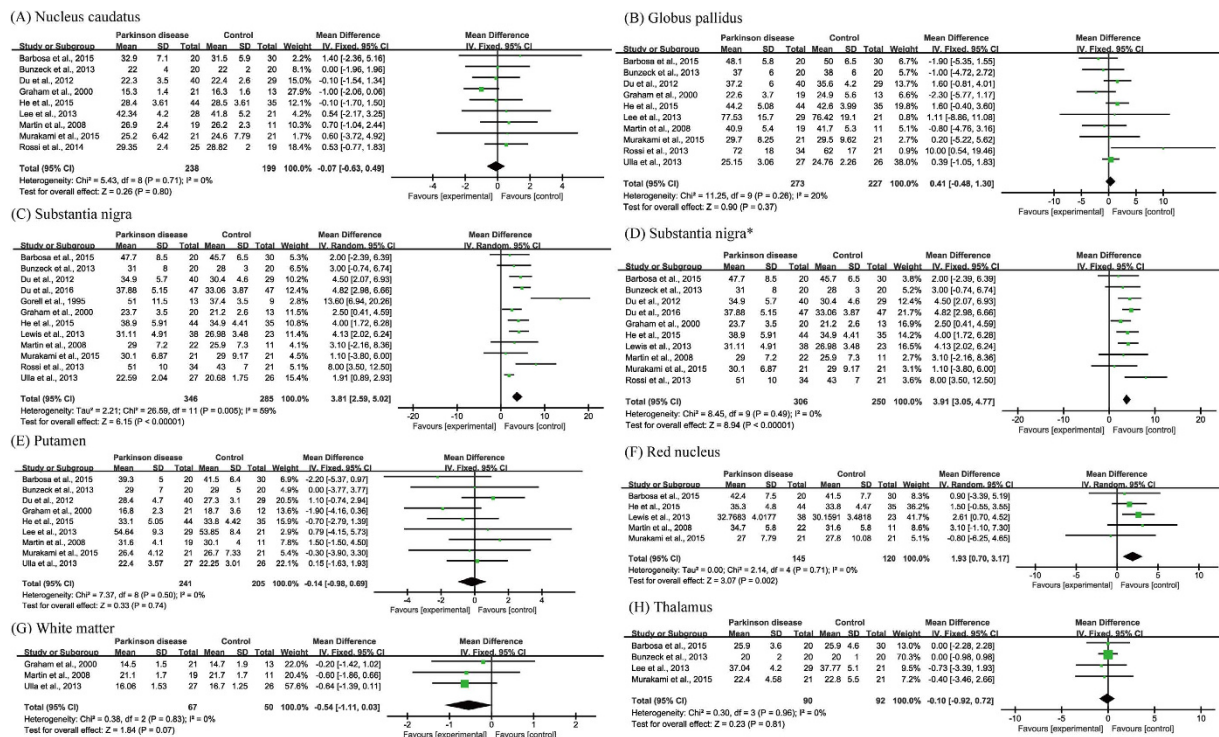


**Figure 4. Statistical summaries and forest plots of studies comparing iron concentrations by MRI R2\* relaxometry. (C) Pooled using random-effects models. The others were pooled using fixed-effects models. \* Analyzed after heterogeneity was removed.**

results of either postmortem or R2\* meta-analyses did not display significant difference, which was in line with the mixed trends of changes in individual studies.

**Nucleus caudatus.** Similar to globus pallidus, both postmortem and R2\* meta-analyses returned no significant difference with mixed trends in iron content in the individual studies. Results of pooled SWI analysis showed a significant increase of iron content in PD patients. There were six studies that showed a significant<sup>31,37</sup> or a trend of increase<sup>33–36</sup> in iron levels in the nucleus caudatus while only one study suggested a trend of decrease<sup>34</sup>.

**Frontal lobe, temporal lobe and cerebellum.** Although postmortem results of these structures were available, the pooled sample sizes were small (98, 44 and 58, respectively). All the four studies on frontal lobe<sup>2,11,12,14</sup> and two on cerebellum<sup>2,14</sup> reported negative results. Although one article reported a significant decrease of iron levels in the temporal lobe<sup>17</sup>, two studies showed no change<sup>11,13</sup>. Further studies were needed to clarify iron levels in these structures.

**Red nucleus.** No available studies using postmortem samples fit our criteria. Results of R2\* and SWI pooled analyses suggested an increase of iron levels in the red nucleus. For the R2\* analyses, four studies reported a significant increase<sup>3</sup> or an increasing trend<sup>20,27,29</sup>, whereas one showed a decreasing trend<sup>30</sup>. For the SWI analyses, seven out of eight studies reported no remarkable changes, among which three showed a decreasing trend<sup>32,34,38</sup> and one an increasing trend in iron content<sup>32,36–38</sup>. In comparison, the study that showed significantly elevated iron content in PD patients<sup>33</sup> drove roughly half of the total effect size (Fig. 6H). Noteworthy, two PD groups (advanced and mild disease stage) were included in this study that had the same control group<sup>33</sup>. The advanced PD group was chosen for the current analysis to compare with postmortem samples that are usually obtained at late stage PD. When the mild group was included, results of SWI meta-analyses were not affected except in the red nucleus. There was no significant increase of iron content detected (Figs S1 and S2), suggesting that the severity of PD might be a factor affecting iron deposits in the red nucleus. As a note, the mild stage in this study<sup>33</sup> was Hoehn and Yahr scale <1.5, which appeared milder than normally defined.

**Thalamus and white matter.** No qualified study using postmortem samples was available. Results of both R2\* and SWI meta-analyses suggested no association of iron levels with PD in the thalamus and white matter of the brain. Furthermore, all of the selected individual studies<sup>31,34–37</sup> returned negative results.

**Discussion**

Iron dysregulation is frequently associated with neurodegenerative disorders, including Huntington disease, Alzheimer's disease, amyotrophic lateral sclerosis, and frontotemporal lobar degeneration<sup>40,41</sup>. Nonetheless, it remains unclear whether such defect is a cause or a consequence of neurodegeneration. A large body of evidence

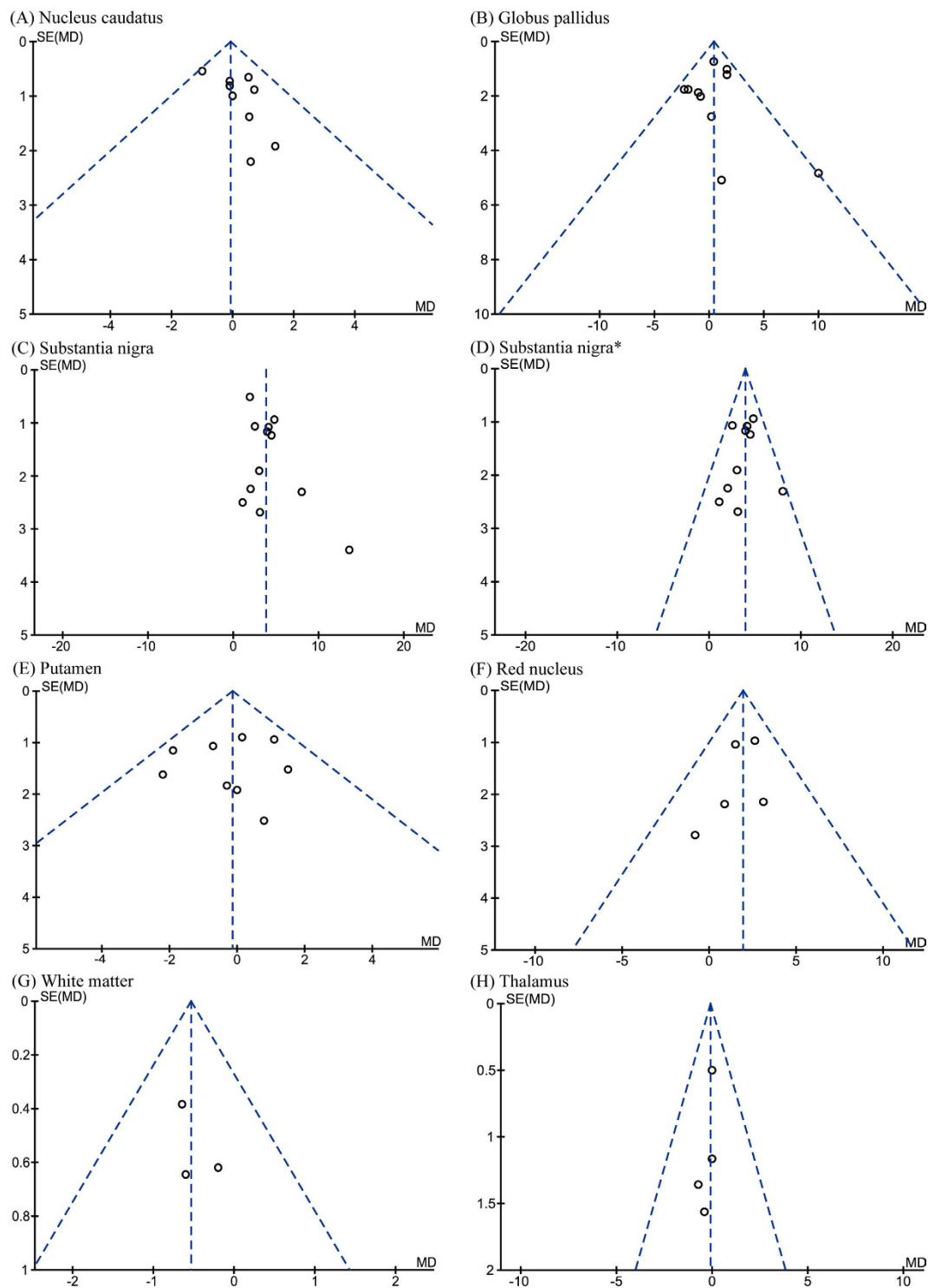


**Figure 5.** Funnel plots that examine possible publication bias in the studies by  $R2^*$ . \*Analyzed after heterogeneity was removed.

suggests abnormal iron levels in the brains of PD patients and a role for iron dysregulation in PD pathogenesis<sup>42–44</sup>. Our study represents the first meta-analysis that systematically assesses iron levels in various brain regions of PD patients by postmortem measurements and by MRI ( $R2^*$  and SWI). Our analysis confirms a perturbed iron homeostasis in the substantia nigra and suggests that an increase in iron levels may also occur in the putamen and red nucleus (Table 2).

Some caveats in regard to the scope of this meta-analysis must be taken into account. First, in the postmortem analyses different iron quantification methods (SPH, AA, COL, ICP and MS) have been used. The differential sensitivity and specificity of these methods may contribute to an elevated heterogeneity. Second, disease stage and

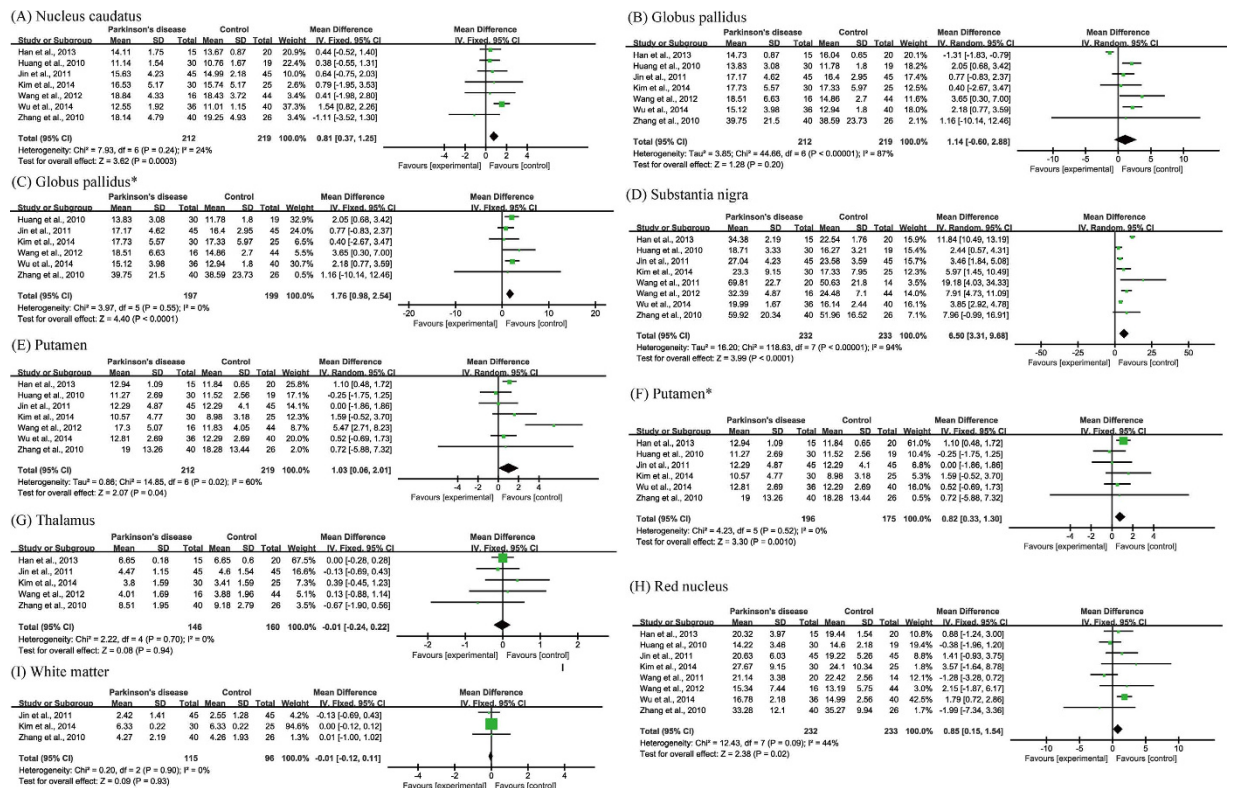


**Figure 6. Statistical summaries and forest plots of studies comparing iron concentrations by SWI relaxometry. (B,D,E) Pooled using random-effects models. The others were pooled using fixed-effects models. \* Analyzed after heterogeneity was removed.**

age may be two influencing factors when evaluating iron concentration in the brain<sup>40,45,46</sup>, which unfortunately is not addressed in the current study due to incomplete information and limited sample size. For example, the inclusion of a sub-group of mild-stage PD patients results in a loss of significance in iron levels in the red nucleus of SWI meta-analysis.

It is well recognized that iron overload contributes to oxidative stress through Fenton reaction, promoting the death of dopaminergic neurons in the substantia nigra<sup>47</sup>. Such iron accumulation is known to be associated with increased ferritin and neuromelanin iron loads<sup>48,49</sup>, as well as increased expression of divalent metal transporter 1 that may contribute to PD pathogenesis via its capacity of transporting ferrous iron<sup>47</sup>. Furthermore, aggregation of  $\alpha$ -synuclein can be accelerated when bound with free iron<sup>50</sup>. However, it remains unclear whether iron deposit triggers or accelerates neurodegeneration, or if they are a secondary event due to neuronal degeneration. Therefore, it is important to determine the timing of iron deposit in substantia nigra during the pathogenesis of PD. Because postmortem measurements are usually made in a very late stage of PD, future longitudinal studies of iron contents are warranted<sup>47</sup>. Consistent results obtained from postmortem, R2\*, and SWI measurements suggest that longitudinal evaluation of iron content in the substantia nigra can be appropriately made by MRI methods.

It appears that the MRI methods of R2\* and SWI do not completely match the postmortem results, presumably the latter being the standard. Iron deposit is detected by SWI in the globus pallidus and nucleus caudatus, but these are inconsistent with the postmortem observations. Results from R2\* studies also suggest an inconsistency in the putamen as both postmortem and SWI effects show an iron overload. Loss of striatal dopamine in PD is most prominent in sub-regions of the putamen<sup>51</sup>, which may be associated with an increase in iron levels. However, this may be a weak argument considering that the postmortem iron increase in this structure is driven by a single study as noted in the Results. It has previously been proposed that SWI is more specific and precise than other methods to estimate brain iron content<sup>52</sup>. Our results suggest that both methods have weakness in measuring iron content. The iron signal determined by R2\* may be disrupted by calcification<sup>53</sup> and lipid content<sup>54</sup>, and the output value is a weighted summation of magnetic properties from both local and surrounding tissues<sup>28</sup>. Intrinsic defects of SWI include a difficulty in distinguishing diamagnetic and paramagnetic susceptibility owing to the convoluting effect of the dipole fields<sup>55</sup>. There are also limitations of MRI *per se*, such that myelin, especially small myelinated fibers, cannot be easily distinguishable from iron deposition<sup>46</sup>, and the phase value of MRI reflects not only non-heme iron deposited in the tissue but also the heme iron in hemosiderin or in circulating blood<sup>56</sup>. Microbleeds may also be a confounding factor especially when brain iron content is estimated in older adults<sup>57</sup>. Given the MRI phase's nonlocal behavior, one should pay attention to the signal interference of adjacent structures. For example, the red nucleus lies adjacent to substantia nigra in the midbrain and is likely high in iron levels due to its proximity<sup>58</sup>. In other words, the differences detected in iron levels in the red nucleus may arise from the adjacent substantia nigra, instead of from the structure itself. Increased iron levels in red nucleus are



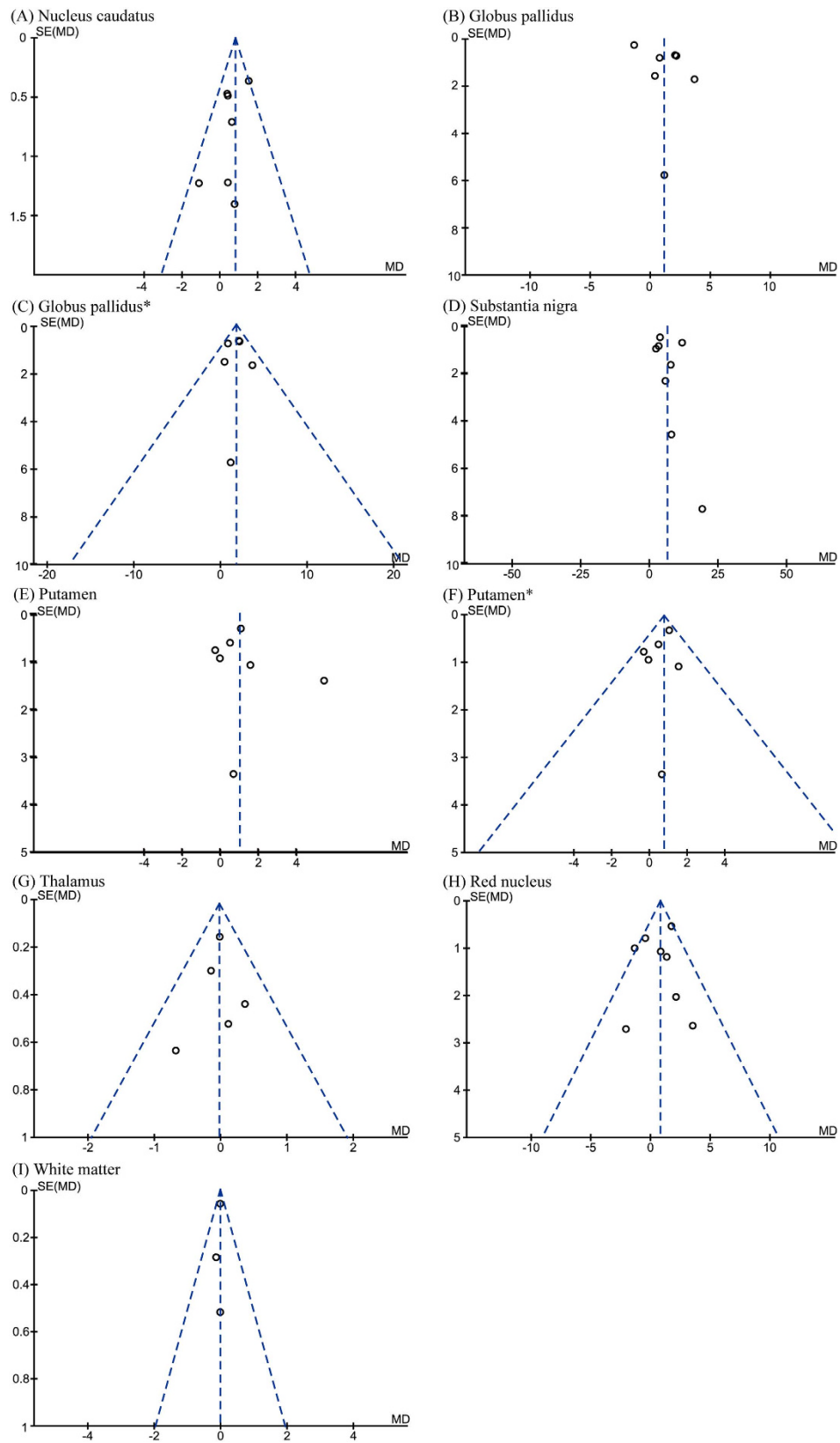


**Figure 7.** Funnel plots that examine possible publication bias in the studies by SWI. \*Analyzed after heterogeneity was removed.

associated with levodopa-induced dyskinesia of PD<sup>3</sup>. Future postmortem studies are warranted to confirm iron deposit in this structure. This is also the case for the putamen and globus pallidus, due to their relative proximity.

	Postmortem			R2*			SWI		
	Change	p	n	Change	p	n	Change	p	n
Substantia nigra	↑	0.01	173	↑	<10 <sup>-5</sup>	631	↑	<10 <sup>-4</sup>	465
	↑ <sup>a</sup>	0.004	161	↑ <sup>a</sup>	<10 <sup>-5</sup>	556			
Putamen	↑	0.002	100	—	0.74	446	↑	0.04	431
							↑ <sup>a</sup>	0.001	371
Globus pallidus	—	0.72	104	—	0.37	500	—	0.20	431
							↑ <sup>a</sup>	<10 <sup>-4</sup>	396
Nucleus caudatus	—	0.47	117	—	0.80	437	↑	0.0003	431
Frontal lobe	—	0.33	98	NA	NA	NA	NA	NA	NA
Temporal lobe	—	0.11	44	NA	NA	NA	NA	NA	NA
Cerebellum	—	0.14	58	NA	NA	NA	NA	NA	NA
Red nucleus	NA	NA	NA	↑	0.002	265	↑	0.02	465
Thalamus	NA	NA	NA	—	0.81	182	—	0.94	306
White matter	NA	NA	NA	—	0.07	117	—	0.93	211

**Table 2.** A summary of changes in brain iron levels of PD patients based on the current meta-analysis.

↑Increased iron level in PD. —No change of iron level in PD. NA, no data available. <sup>a</sup>Analyzed after heterogeneity was removed.

Recently, quantitative susceptibility mapping (QSM), a potentially superior method to measuring iron content *in vivo*, has been applied to measure PD-related iron deposition and progression<sup>28</sup>. By this method, Guan *et al.*<sup>59</sup> have recently reported a distinct pattern of iron accumulation according to disease stage, with iron spreading from the substantia nigra in early stages to the substantia nigra, red nucleus and globus pallidus in later stages. This could explain the aforementioned discrepancy in the red nucleus when the mild PD group is included, as well as provide a potential explanation for inconsistent findings between neuropathology and MRI techniques.

In conclusion, the current meta-analysis corroborates iron overload in substantia nigra and suggests such iron homeostasis defect in the putamen (by postmortem and SWI, but not R2\*) and the red nucleus (by R2\* and SWI; no data by postmortem) of PD patients. Both the R2\* or SWI techniques may not authentically reflect iron changes in brain regions other than substantia nigra. Our results offer a comprehensive understanding of iron loads in different brain regions in association with PD, and contribute to the evaluation of measuring accuracy of iron concentration by MRI methods.

## Methods

**Literature Search Strategy.** Literature related to iron and Parkinson's disease were searched in four databases including Medline via PubMed, Web of Science, the Cochrane Central Register of Controlled Trials (CENTRAL) and Embase via OVID, dated till 19<sup>th</sup> November 2015. The keywords for iron and Parkinson's disease are “iron” or “Fe” and “Parkinson disease”, “Parkinson's disease”, “Parkinsons disease” or “Parkinsonian”, respectively.

**Study Selection.** Based on the keywords, titles and abstracts of the identified publications were screened. Following an exhaustive examination of the literature contents, articles were included according to our selection criteria: population (idiopathic PD patients), comparators (individuals free of neurological disorders), outcome measurement (iron content in brain regions), and language (articles written in English or Chinese). Review articles, qualitative and semi-quantitative studies were excluded.

**Data Extraction.** The literature search and data extraction were conducted by two researchers (Qing-Qing Zhuang and Jian-Yong Wang) independently. In the case of a dispute, a third investigator was included to discuss and reach an agreement. The following data was extracted: sample size, age, sex, PD diagnosis, iron detection methods, the type of samples, clinical scores, and iron content or R2\* value or phase value in brain regions. Assessment of the detailed information was listed in Table 1. As shown in this table, the disease severity (Hoehn and Yahr scale) was not provided by all the included studies and the provided else information was also varied in forms including UPDRS score, UPDRS motor score, and/or disease duration. Therefore, we did not include the disease severity as a source of variance in the analysis.

Iron quantification methods employed in the postmortem study of brain samples included spectrophotometry (SPH), atomic absorption (AA), colorimetry (COL), inductively coupled plasma spectroscopy (ICP) and Mössbauer spectroscopy (MS). To be consistent in brain weights, a conversion of dry weight to wet weight was applied based on a dry/wet ratio as suggested in previous studies<sup>60,61</sup>. The SWI signal phase is orientation-dependent and nonlocal<sup>55</sup>. As a result, the phase value appears to be either positively or negatively correlated with iron concentration depending on the orientation relative to the Bo field<sup>62</sup>. Thus, a conversion from SWI phase value to iron concentration was applied based on formulas suggested in previous studies<sup>35,36</sup>; that is, concentration = 397.72 × (phase value) + 3.4097 (extracted from Fig. 1 of ref. 36) for the studies of positive setting<sup>31,34,36</sup>, and concentration = -128.23 × (phase value) + 3.1897 (extracted from Fig. 2 of ref. 35) for the studies of negative setting<sup>32,33,35,37,38</sup>.

**Quality Assessment.** The Newcastle-Ottawa Scale<sup>63</sup> was employed to assess the quality of the chosen studies. This tool classified studies in three broad perspectives: selection of the study groups, comparability of the groups, and ascertainment of either exposure or outcome of interest for the studies. Semi-quantitative measurement using a star system assesses the quality of study. The highest quality studies can get a maximum of nine stars.

**Statistical Analysis.** Eleven postmortem analysis and 22 MRI analysis articles were eventually selected for our meta-analysis. Means, standard deviations (or standard errors), and the number of samples were extracted in each study. Meta-analyses were conducted within the studies of the same brain region after sorting into their respective quantitative groups of postmortem analysis, R2\* and SWI. In the case that the same data appeared in multiple studies, the data were used only once. All of the analyses were performed using Review Manager 5.2 for Windows (<http://ims.cochrane.org/revman>). A two-tailed *p* value <0.05 was considered statistically significant. Weighted mean difference (WMD) was regarded as an effect size. Q-statistics and I<sup>2</sup> were used for assessing the heterogeneity<sup>64,65</sup>. A random effects model was applied when heterogeneity was found by Q-statistics or when I<sup>2</sup> > 50%. A fixed effects model was applied otherwise.

## References

- Dexter, D. T. *et al.* Alterations in the levels of iron, ferritin and other trace metals in Parkinson's disease and other neurodegenerative diseases affecting the basal ganglia. *Brain* **114** (Pt 4), 1953–1975 (1991).
- Dexter, D. T. *et al.* Increased nigral iron content and alterations in other metal ions occurring in brain in Parkinson's disease. *J Neurochem* **52**, 1830–1836 (1989).
- Lewis, M. M. *et al.* Higher iron in the red nucleus marks Parkinson's dyskinesia. *Neurobiol Aging* **34**, 1497–1503 (2013).
- Riederer, P. *et al.* Transition metals, ferritin, glutathione, and ascorbic acid in parkinsonian brains. *J Neurochem* **52**, 515–520 (1989).
- Hardy, P. A. *et al.* Correlation of R2 with total iron concentration in the brains of rhesus monkeys. *J Magn Reson Imaging* **21**, 118–127 (2005).
- Langkammer, C. *et al.* Quantitative MR Imaging of Brain Iron: A Postmortem Validation Study. *Radiology* **257**, 455–462 (2010).
- Ordidge, R. J., Gorell, J. M., Deniau, J. C., Knight, R. A. & Helpert, J. A. Assessment of relative brain iron concentrations using T2-weighted and T2\*-weighted MRI at 3 Tesla. *Magn Reson Med* **32**, 335–341 (1994).
- Pyatigorskaya, N., Gallea, C., Garcia-Lorenzo, D., Vidailhet, M. & Lehericy, S. A review of the use of magnetic resonance imaging in Parkinson's disease. *Ther Adv Neurol Disord* **7**, 12–26 (2014).
- Chen, J. C. *et al.* MR of human postmortem brain tissue: correlative study between T2 and assays of iron and ferritin in Parkinson and Huntington disease. *Am J Neuroradiol* **14**, 275–281 (1993).
- Galazka-Friedman, J. *et al.* Iron in parkinsonian and control substantia nigra—a Mossbauer spectroscopy study. *Mov Disord* **11**, 8–16 (1996).
- Griffiths, P. D. & Crossman, A. R. Distribution of iron in the basal ganglia and neocortex in postmortem tissue in Parkinson's disease and Alzheimer's disease. *Dementia* **4**, 61–65 (1993).
- Loeffler, D. A. *et al.* Transferrin and iron in normal, Alzheimer's disease, and Parkinson's disease brain regions. *J Neurochem* **65**, 710–724 (1995).
- Sofic, E. *et al.* Increased iron (III) and total iron content in post mortem substantia nigra of parkinsonian brain. *J Neural Transm* **74**, 199–205 (1988).
- Uitti, R. J. *et al.* Regional metal concentrations in Parkinson's disease, other chronic neurological diseases, and control brains. *Can J Neurol Sci* **16**, 310–314 (1989).
- Visanji, N. P. *et al.* Iron deficiency in parkinsonism: region-specific iron dysregulation in Parkinson's disease and multiple system atrophy. *J Parkinsons Dis* **3**, 523–537 (2013).
- Wypijewska, A. *et al.* Iron and reactive oxygen species activity in parkinsonian substantia nigra. *Parkinsonism Relat Disord* **16**, 329–333 (2010).
- Yu, X. *et al.* Decreased iron levels in the temporal cortex in postmortem human brains with Parkinson disease. *Neurology* **80**, 492–495 (2013).
- Gorell, J. M. *et al.* Increased iron-related MRI contrast in the substantia nigra in Parkinson's disease. *Neurology* **45**, 1138–1143 (1995).
- Graham, J. M., Paley, M. N., Grunewald, R. A., Hoggard, N. & Griffiths, P. D. Brain iron deposition in Parkinson's disease imaged using the PRIME magnetic resonance sequence. *Brain* **123** Pt 12, 2423–2431 (2000).
- Martin, W. R. W., Wieler, M. & Gee, M. Midbrain iron content in early Parkinson disease - A potential biomarker of disease status. *Neurology* **70**, 1411–1417 (2008).
- Du, G. *et al.* Serum iron and ferritin level in idiopathic Parkinson. *Pak J Biol Sci* **15**, 1094–1097 (2012).
- Bunzeck, N. *et al.* Motor phenotype and magnetic resonance measures of basal ganglia iron levels in Parkinson's disease. *Parkinsonism Relat Disord* **19**, 1136–1142 (2013).
- Lee, M. F. *et al.* N-acetylcysteine (NAC) inhibits cell growth by mediating the EGFR/Akt/HMG box-containing protein 1 (HBP1) signaling pathway in invasive oral cancer. *Oral Oncol* **49**, 129–135 (2013).
- Rossi, M., Ruottinen, H., Soimakallio, S., Elovaara, I. & Dastidar, P. Clinical MRI for iron detection in Parkinson's disease. *Clin Imaging* **37**, 631–636 (2013).
- Ulla, M. *et al.* Is R2\* a new MRI biomarker for the progression of Parkinson's disease? A longitudinal follow-up. *PLoS One* **8**, e57904 (2013).
- Rossi, M. E., Ruottinen, H., Saunamäki, T., Elovaara, I. & Dastidar, P. Imaging brain iron and diffusion patterns: a follow-up study of Parkinson's disease in the initial stages. *Acad Radiol* **21**, 64–71 (2014).
- Barbosa, J. H. O. *et al.* Quantifying brain iron deposition in patients with Parkinson's disease using quantitative susceptibility mapping, R2 and R2. *Magn Reson Imaging* **33**, 559–565 (2015).
- Du, G. *et al.* Quantitative susceptibility mapping of the midbrain in Parkinson's disease. *Mov Disord* **31**, 317–324 (2016).
- He, N. *et al.* Region-specific disturbed iron distribution in early idiopathic Parkinson's disease measured by quantitative susceptibility mapping. *Hum Brain Mapp* **36**, 4407–4420 (2015).
- Murakami, Y. *et al.* Usefulness of quantitative susceptibility mapping for the diagnosis of Parkinson disease. *Am J Neuroradiol* **36**, 1102–1108 (2015).
- Han, Y. H. *et al.* Topographical differences of brain iron deposition between progressive supranuclear palsy and parkinsonian variant multiple system atrophy. *J Neurol Sci* **325**, 29–35 (2013).
- Wang, C. *et al.* Application of quantitative measurement on midbrain in Parkinson disease with MR susceptibility-weighted imaging. *Chin J Med Imaging Technol* **27**, 1129–1133 (2011).

33. Wu, S. F. *et al.* Assessment of cerebral iron content in patients with Parkinson's disease by the susceptibility-weighted MRI. *Eur Rev Med Pharmacol Sci* **18**, 2605–2608 (2014).
34. Zhang, J. *et al.* Characterizing iron deposition in Parkinson's disease using susceptibility-weighted imaging: an *in vivo* MR study. *Brain Res* **1330**, 124–130 (2010).
35. Jin, L. *et al.* Decreased serum ceruloplasmin levels characteristically aggravate nigral iron deposition in Parkinson's disease. *Brain* **134**, 50–58 (2011).
36. Kim, T. H. & Lee, J. H. Serum uric acid and nigral iron deposition in Parkinson's disease: A pilot study. *Mov Disord* **29**, S88–S88 (2014).
37. Wang, Y. *et al.* Different iron-deposition patterns of multiple system atrophy with predominant parkinsonism and idiopathic Parkinson diseases demonstrated by phase-corrected susceptibility-weighted imaging. *Am J Neuroradiol* **33**, 266–273 (2012).
38. Huang, X. M., Sun, B., Xue, Y. J. & Duan, Q. Susceptibility-weighted imaging in detecting brain iron accumulation of Parkinson's disease. *Zhonghua Yi Xue Za Zhi* **90**, 3054–3058 (2010).
39. Manor, O. & Zucker, D. M. Small sample inference for the fixed effects in the mixed linear model. *Comput Stat Data An* **46**, 801–817 (2004).
40. Ward, R. J., Zucca, F. A., Duyn, J. H., Crichton, R. R. & Zecca, L. The role of iron in brain ageing and neurodegenerative disorders. *Lancet Neurol* **13**, 1045–1060 (2014).
41. Biasotto, G., Di Lorenzo, D., Archetti, S. & Zanella, I. Iron and Neurodegeneration: Is Ferritinophagy the Link? *Mol Neurobiol* **53**, 5542–5574 (2015).
42. Oshiro, S., Morioka, M. S. & Kikuchi, M. Dysregulation of iron metabolism in Alzheimer's disease, Parkinson's disease, and amyotrophic lateral sclerosis. *Adv Pharmacol Sci* **2011**, 378278 (2011).
43. Perry, G. *et al.* The role of iron and copper in the aetiology of neurodegenerative disorders: therapeutic implications. *CNS Drugs* **16**, 339–352 (2002).
44. Sayre, L. M., Perry, G., Atwood, C. S. & Smith, M. A. The role of metals in neurodegenerative diseases. *Cell Mol Biol (Noisy-le-grand)* **46**, 731–741 (2000).
45. Zecca, L., Youdim, M. B., Riederer, P., Connor, J. R. & Crichton, R. R. Iron, brain ageing and neurodegenerative disorders. *Nat Rev Neurosci* **5**, 863–873 (2004).
46. Daugherty, A. & Raz, N. Age-related differences in iron content of subcortical nuclei observed *in vivo*: A meta-analysis. *Neuroimage* **70**, 113–121 (2013).
47. Hadzhieva, M., Kirches, E. & Mawrin, C. Review: iron metabolism and the role of iron in neurodegenerative disorders. *Neuropathol Appl Neurobiol* **40**, 240–257 (2014).
48. Ben-Shachar, D., Riederer, P. & Youdim, M. B. Iron-melanin interaction and lipid peroxidation: implications for Parkinson's disease. *J Neurochem* **57**, 1609–1614 (1991).
49. Jellinger, K., Paulus, W., Grundke-Iqbal, I., Riederer, P. & Youdim, M. B. Brain iron and ferritin in Parkinson's and Alzheimer's diseases. *J Neural Transm Park Dis Dement Sect 2*, 327–340 (1990).
50. Wolozin, B. & Golts, N. Iron and Parkinson's disease. *Neuroscientist* **8**, 22–32 (2002).
51. Kish, S. J., Shannak, K. & Hornykiewicz, O. Uneven pattern of dopamine loss in the striatum of patients with idiopathic Parkinson's disease. Pathophysiologic and clinical implications. *New Engl J Med* **318**, 876–880 (1988).
52. Ogg, R. J., Langston, J. W., Haacke, E. M., Steen, R. G. & Taylor, J. S. The correlation between phase shifts in gradient-echo MR images and regional brain iron concentration. *Magn Reson Imaging* **17**, 1141–1148 (1999).
53. Naderi, S., Colakoglu, Z. & Luleci, G. Calcification of basal ganglia associated with pontine calcification in four cases: a radiologic and genetic study. *Clin Neurol Neurosurg* **95**, 155–157 (1993).
54. He, X. & Yablonskiy, D. A. Biophysical mechanisms of phase contrast in gradient echo MRI. *Proc Natl Acad Sci USA* **106**, 13558–13563 (2009).
55. Liu, C., Li, W., Tong, K. A., Yeom, K. W. & Kuzminski, S. Susceptibility-weighted imaging and quantitative susceptibility mapping in the brain. *J Magn Reson Imaging* **42**, 23–41 (2015).
56. Anderson, C. M. *et al.* Brain T2 relaxation times correlate with regional cerebral blood volume. *MAGMA* **18**, 3–6 (2005).
57. Penke, L. *et al.* Brain iron deposits are associated with general cognitive ability and cognitive aging. *Neurobiol Aging* **33**, 510–517 (2012).
58. Drayer, B. *et al.* MRI of brain iron. *Am J Roentgenol* **147**, 103–110 (1986).
59. Guan, X. *et al.* Regionally progressive accumulation of iron in Parkinson's disease as measured by quantitative susceptibility mapping. *NMR Biomed*, doi: 10.1002/nbm.3489 (2016).
60. Schrag, M., Mueller, C., Oyoyo, U., Smith, M. A. & Kirsch, W. M. Iron, zinc and copper in the Alzheimer's disease brain: a quantitative meta-analysis. Some insight on the influence of citation bias on scientific opinion. *Prog Neurobiol* **94**, 296–306 (2011).
61. House, M. J. *et al.* Correlation of proton transverse relaxation rates (R2) with iron concentrations in postmortem brain tissue from alzheimer's disease patients. *Magn Reson Med* **57**, 172–180 (2007).
62. Yablonskiy, D. A. & Haacke, E. M. Theory of NMR signal behavior in magnetically inhomogeneous tissues: the static dephasing regime. *Magn Reson Med* **32**, 749–763 (1994).
63. Stang, A. Critical evaluation of the Newcastle-Ottawa scale for the assessment of the quality of nonrandomized studies in meta-analyses. *Eur J Epidemiol* **25**, 603–605 (2010).
64. Cochran, W. G. The combination of estimates from different experiments. *Biometrics* **10**, 101–129 (1954).
65. Higgins, J. P. T. & Thompson, S. G. Quantifying heterogeneity in a meta-analysis. *Stat Med* **21**, 1539–1558 (2002).
66. Calne, D. B., Snow, B. J. & Lee, C. Criteria for diagnosing Parkinson's disease. *Ann Neurol* **32** Suppl, S125–S127 (1992).
67. Hughes, A. J., Daniel, S. E., Blankson, S. & Lees, A. J. A clinicopathologic study of 100 cases of Parkinson's disease. *Arch Neurol* **50**, 140–148 (1993).
68. Gibb, W. R. & Lees, A. J. The relevance of the Lewy body to the pathogenesis of idiopathic Parkinson's disease. *J Neurol Neurosurg Psychiatry* **51**, 745–752 (1988).

## Acknowledgements

The authors appreciate Drs Jennifer Harr and Wen-Hsing Cheng for critical help improving readability and accuracy of the manuscript. This work was supported by funding from Zhejiang Provincial Natural Science Foundation (LY16H250003, LY16H260003, and LR13H020002), National Natural Science Foundation of China (81571087), and Wenzhou Science and Technology Bureau (Y20150005).

## Author Contributions

J.Y.W. and Q.Q.Z. performed the data collection, extraction and analyses, L.B.Z., H.Z., T.L., R.L. and S.F.C. contributed to partial data extraction and interpretation, X.Z., C.P.H. and J.H.Z. designed and supervised the study, J.Y.W., Q.Q.Z. and J.H.Z. wrote the manuscript. All authors read and approved the final manuscript.

## Additional Information

**Supplementary information** accompanies this paper at <http://www.nature.com/srep>

**Competing financial interests:** The authors declare no competing financial interests.

**How to cite this article:** Wang, J.-Y. *et al.* Meta-analysis of brain iron levels of Parkinson's disease patients determined by postmortem and MRI measurements. *Sci. Rep.* **6**, 36669; doi: 10.1038/srep36669 (2016).

**Publisher's note:** Springer Nature remains neutral with regard to jurisdictional claims in published maps and institutional affiliations.



This work is licensed under a Creative Commons Attribution 4.0 International License. The images or other third party material in this article are included in the article's Creative Commons license, unless indicated otherwise in the credit line; if the material is not included under the Creative Commons license, users will need to obtain permission from the license holder to reproduce the material. To view a copy of this license, visit <http://creativecommons.org/licenses/by/4.0/>

© The Author(s) 2016